JOURNAL OF IRON AND STEEL RESEARCH, INTERNATIONAL. 2013, 20(12): 00-00

Effects of Welding Procedure on Corrosion Resistance and Hydrogen Embrittlement of Supermartensitic Stainless Steel Deposits

Zappa Sebastián[1], Surian Estela[1,2], Svoboda Hernán[3,4]

(1. Research Secretariat, Faculty of Engineering, National University of Lomas de Zamora, Lomas de Zamora 1832, Buenos Aires, Argentina; 2. Deytema-Development and Technology of Materials Centre, Regional Faculty San Nicolás, National Technological University, San Nicolás 2900, Buenos Aires, Argentina; 3. Materials and Structures Laboratory, Intecin, Faculty of Engineering, National University of Buenos Aires, CABA 1127, Buenos Aires, Argentina; 4. Conicet-National Scientific and Technical Research Council, CABA 1033, Buenos Aires, Argentina)

Abstract: The effects of shielding gas and post weld heat treatment on the pitting resistance, stress corrosion cracking and hydrogen embrittlement of supermartensitic stainless steel deposits were studied. Two all-weld-metal test coupons were prepared using a metal-cored wire under Ar+5%He and Ar+18%CO_2 gas shielding mixtures. Solubilizing and solubilizing plus double tempering heat treatments were done with the objective of achieving different microstructural results. The samples welded under Ar+5%He showed higher pitting corrosion resistance, for all post weld heat treatments, than those welded under Ar+18%CO_2. The different post weld heat treatments generated higher susceptibility to this corrosion mechanism. None of the samples presented signs of stress corrosion cracking, but in those subjected to the heat treatment, grain boundary selective attack was observed, on the surfaces of all the samples studied. The samples with highest hardness were the more susceptible to hydrogen damage, thereby leading to reduced tensile strength on this condition.

Key words: supermartensitic stainless steel; shielding gas; post weld heat treatment; corrosion; hydrogen embrittlement

Supermartensitic stainless steels (SMSS) offer good corrosion resistance in sweet and slightly acid environments and have been developed for OCTG (oil country tubular goods) applications[1]. Since the middle of the 1990's, welding procedures for SMSS are available and their utilization, almost exclusively in the oil and gas industry, has markedly increased[2]. They also offer high strength and good toughness at low temperature through the application of post weld heat treatments[3]. In the last times, the development of SMSS consumables has been focused and several research programs are working on to understand their behavior in different applications[4-5].

It is known that post weld heat treatment (PWHT) at 1000 ℃ with double tempering eliminates the ferrite, tempers martensite and maximizes the content of retained austenite in the microstructure at room temperature[6]. The combination of these factors is ideal to maximize the toughness of the weld SMSS deposits[6]. The mechanism through which austenite becomes stable after a double tempering can be explained by the thermal instability of the austenite generated during the first tempering[3,7]. The austenite is stable at room temperature due to two causes: the chemical composition and a structural factor associated with a high density of dislocations in the substructure[3,7-8]. The phenomenon of sensitization generates areas with the lower chromium content, due to the precipitation of carbides/carbonitrides of Cr in the heat affected zone (HAZ), particularly after the heat treatment used to generate the tempering of martensite; these regions are more susceptible to the pitting corrosion (PC)[9]. Molybdenum, chromium and carbon contents also affect susceptibility to this type of corrosion[9]. Furthermore, although the SMSS have good corrosion behavior in sweet media (CO_2) and slight-

Biography: Zappa Sebastián(1978—), Male, Doctor; **E-mail**: zappasebastian@hotmail.com; **Received Date**: November 30, 2012

ly sour (low levels of H_2S) environments, the occurrence of intergranular stress corrosion cracking (IGSCC) in the HAZ of supermartensitic steel welds under certain environmental conditions has been reported[10]. The initiation and propagation of this failure mechanism is usually produced by the decrease of chromium content in the adjacency of the grain boundary in the HAZ formed by welding[1,10-11]. Other researchers[12] justify this behavior via a phenomenon of sensitization due to the reduction of chromium content by carbides precipitation[12]. However, other studies[1] reported that the stress corrosion cracking begins in the areas with decreased Cr associated with a phenomenon of oxidation during the welding process. In this regard, aspects related to the welding process as the type of shielding gas used can generate variations in the chemical composition of the deposited metal[13], which can affect its mechanical properties[13] and its corrosion resistance. The mentioned chemical composition variations can be accompanied by changes in the phase′s distribution in the microstructure[14].

In spite of the fact that stress corrosion cracking (SCC) and hydrogen embrittlement (HE) in welded joints have been frequently studied, there is not enough information about these problems in consumable all-weld metal[5,15-16].

The objective of this work was to evaluate the effect of shielding gas and PWHT on the pitting corrosion resistance (PCR), stress corrosion cracking and hydrogen embrittlement in SMSS all-weld metal (AWM) obtained using a metal cored (MC) wire for semiautomatic welding process under gas shielding.

1 Experimental Procedure

Two AWM test coupons were welded according to the standard ANSI/AWS A5.22-95[17], using a ϕ1.2 mm SMSS metal-cored wire under Ar-5% He (H samples) and Ar-18% CO_2 (C samples) shielding gas mixtures, with a gas flow of 18 L/min and stick-out of 20 mm, in the flat position, with the similar heat input, using a semiautomatic welding process. Preheating and interpass temperatures were 100 ℃. The plates were buttered with the consumable to be tested following the mentioned standard[17]. The welding parameters used, in both cases, were voltage of 30 V, current of 300 A, welding speed of 5.5 mm/s, and heat input of 1.6 kJ/mm.

Both welded coupons were evaluated by radiographic testing according to the standard ANSI B31.3：1996[18]. Low level of defects was found.

In transverse cross-sections of each coupon, chemical compositions of all weld metal were determined by means of optical emission spectrometry (OES) measurements except C, N, O and S contents which were analyzed via LECOTM. Microstructural characterization was done using both optical microscopy (OM) scanning electron microscopy (SEM) and X-ray diffraction (XRD). Ferrite contents were measured following the standard ASTM E562-99[19], by quantitative metallography and austenite contents were determined by means of the direct peak comparison method, based on XRD patterns[20].

The objective of these heat treatments was to totally eliminate ferrite from the AWM (product of the incomplete ferrite to austenite transformation) and to maximize austenite fraction. Solubilizing temperatures between 950 and 1050 ℃ assures the dissolution of ferrite and austenite phases with which a 100% martensite microstructure can be obtained[21]. Solubilizing treatments at 1000 ℃ for 1 h, followed by the first tempering at 650 ℃ for 15 min and the second at 600 ℃ for 15 min, have the objective of complete elimination of residual ferrite and obtaining a final martensitic structure with a high content of retained austenite[21-22].

To study pitting corrosion resistance, potentiodynamic polarization curves were drawn with sweep rate of 1 mV/s, and tension range from −0.6 to 0.4 V, in a 2.7 mol/L NaCl solution deaerated with N_2 before using. The electrochemical measurements were done using a three−electrode cell. A saturated calomel electrode and a Pt sheet were used as the reference and counter electrodes, respectively. The work electrodes were made with epoxy resin and wet grounded with 240 and 600-grit SiC, rinsed and dried. Results were recorded with an EG&G Princeton Applied Research model 273 A potentiostat-galvanostat, using flat disc samples with a surface area of 0.7 cm^2 approximately. Due to the stochastic nature of the pitting corrosion tests[23-26], 10 measurements of each condition were performed and averaged. After tests, the samples were analyzed by SEM.

For SCC determinations, three-point bending tests at 100 ℃ in an aqueous solution of 2.7 mol/L NaCl under 1 MPa CO_2 were performed, following the procedure established by the method B of the standard NACE TM 0177-05[27], changing the test medium and the corrosive gas[28]. Longitudinal samples were extracted from the AWM. The specimens were subjected to 90% of the yield stress. The test duration was 720 h. The surface of the specimens for

corrosion tests was not machined after heat treatment, just polished.

To evaluate susceptibility to HE, the samples were tensile loaded at a low velocity strain rate (0.1 mm/min) while hydrogen was cathodic charged during the test. The calibrated area of the test specimen was submerged into a 0.5 mol/L H_2SO_4 solution at 20 ℃ with a constant current density of 20 mA/cm^2.

2 Results

2.1 Chemical composition, microstructure and mechanical properties

Table 1 presents the chemical composition and the ferrite and austenite contents of all weld metal[19-20]. With the double tempering, after solubilizing, the austenite content was increased up to the initial value. The final microstructure obtained consisted of tempered martensite with retained austenite and without ferrite. The mechanism through which austenite increased with the double tempering can be explained by the austenite thermal instability generated by the first tempering[3,7].

Table 1 Chemical composition and ferrite and austenite contents of all weld metal (mass percent, %)

Material	C	Cr	Ni	Mo	Cu	O	N	Ferrite	Austenite
Haw	0.012	12.1	6.27	2.69	0.49	0.39	0.005	10	20
H1000	0.012	12.1	6.27	2.69	0.49	0.39	0.005	0	0
H1000+650+600	0.012	12.1	6.27	2.69	0.49	0.39	0.005	0	21
Caw	0.022	11.9	5.98	2.57	0.43	0.61	0.026	6	18
C1000	0.022	11.9	5.98	2.57	0.43	0.61	0.026	0	0
C1000+650+600	0.022	11.9	5.98	2.57	0.43	0.61	0.026	0	19

Note: Haw and Caw are as welded samples; H1000 and C1000 are those only solubilized at 1000 ℃; H1000+650+600 and C1000+650+600 are the samples after solubilizing plus tempering at 650℃×15 min plus tempering at 600 ℃×15 min.

2.2 Pitting resistance

In Fig. 1 (a), the pitting potential values for the different samples are presented. It can be observed that samples welded under Ar+5%He showed higher pitting corrosion resistance. The different PWHTs generated higher susceptibility to this corrosion mechanism for both shielding gases. Although the differences observed in the pitting potential (E_p) for the two welded samples were small, defined tendencies were observed. The samples welded under Ar+5%He presented the best results.

Fig. 1 (b) shows the relationship between pitting potential and austenite content for the different conditions studied in this present paper. No direct effect of austenite content on Ep was found.

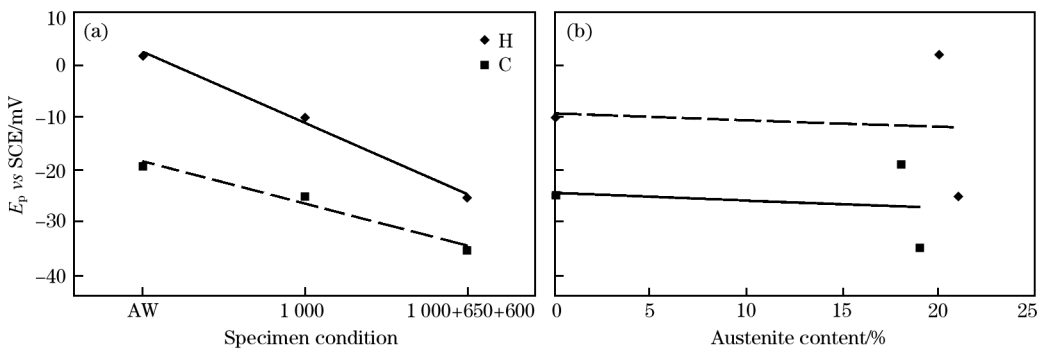

Fig. 1 E_p for different specimens studied (a) and relationship of E_p to austenite content (b)

2.3 SCC tests

The results of SCC tests can be seen in Table 2. None of the as-welded samples presented evidence either of SCC or IGC; all the heat treated samples showed no SCC but grain boundary attack associated with an intergranular corrosion process.

Fig. 2 shows images of IGC for the specimens welded with Ar+18%CO_2 with PWHT. This selective attack morphology was observed in all samples with PWHT but not in AW ones. These results show the strong effect of these heat treatments on IGC susceptibility in this type of materials, in the medium conditions analyzed.

To understand the reason for this type of corrosion,

Table 2 Results of SCC, HE and mechanical property tests

Material	SCC	IGC	Hardness (HV_1)	AR_{air}/%	UTS_{air}/MPa	AR_H/%	UTS_H/MPa	HEI/%
Haw	No	No	324	32.6	1048	8.8	989	73
H1000	No	Yes	318	33.1	986	9.9	945	70
H1000+650+600	No	Yes	293	46.7	941	18.8	890	60
Caw	No	No	348	24.8	1107	5.7	1035	77
C1000	No	Yes	338	28.3	1008	8.2	971	71
C1000+650+600	No	Yes	304	34.5	963	13.5	912	61

Note: IGC—Intergranular corrosion cracking; UTS—Ultimate tensile strength; AR—Area reduction; HEI—hydrogen embrittlement index; subscript air and H means testing in air or under hydrogen charging, respectively.

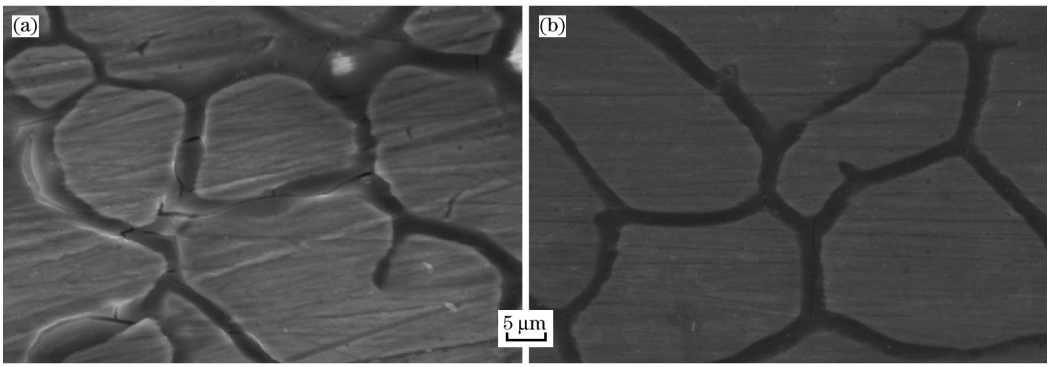

(a) C1000; (b) C1000+650+600.

Fig. 2 IGC in specimens with PWHT

mappings of chemical composition were done in the surface exposed to corrosive environment, in order to demonstrate segregation of certain elements. Fig. 3 shows the mapping of chemical composition made in the unmachined sample C1000+650+600. A large segregation in primary austenitic grain boundary, essentially of Cr, on the surface exposed to corrosion can be seen.

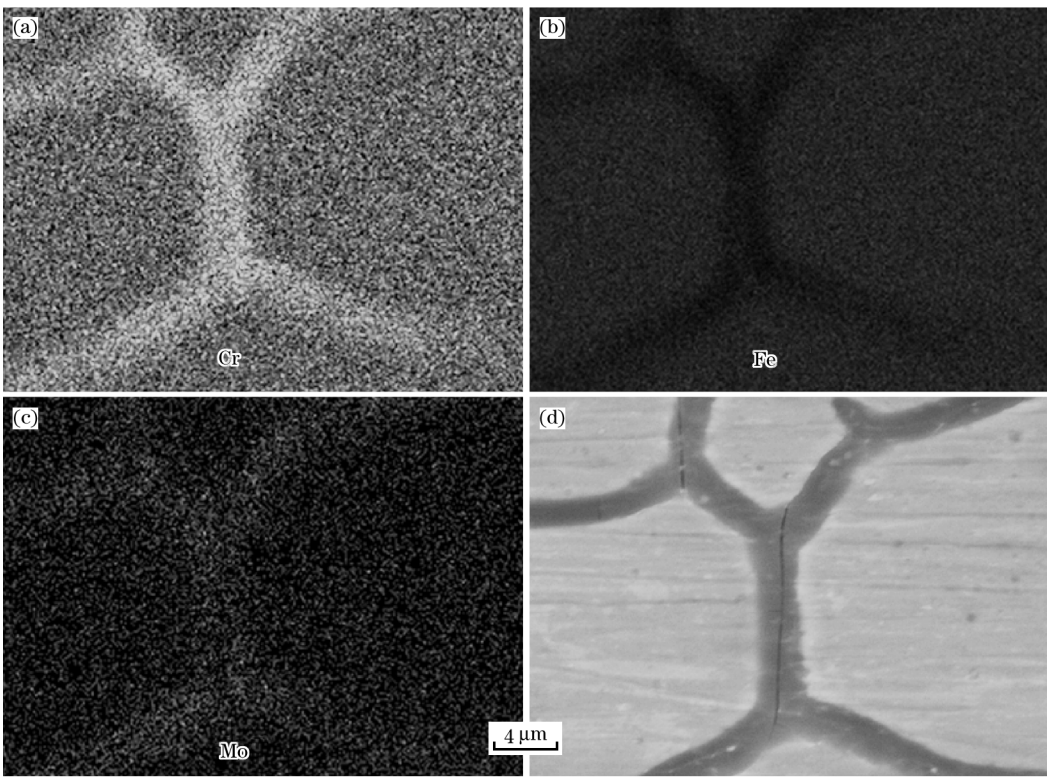

Fig. 3 Mapping of chemical composition in surface exposed to corrosion of unmachined sample C1000+650+600

Similarly, mapping of chemical composition was performed on the samples used for microstructural characterization, where the outer surface after the post weld heat treatment was removed during sample preparation. Fig. 4 shows the mapping of chemical composition performed on the sample C1 000+650+600, machined, where the phenomenon of segregation was not observed.

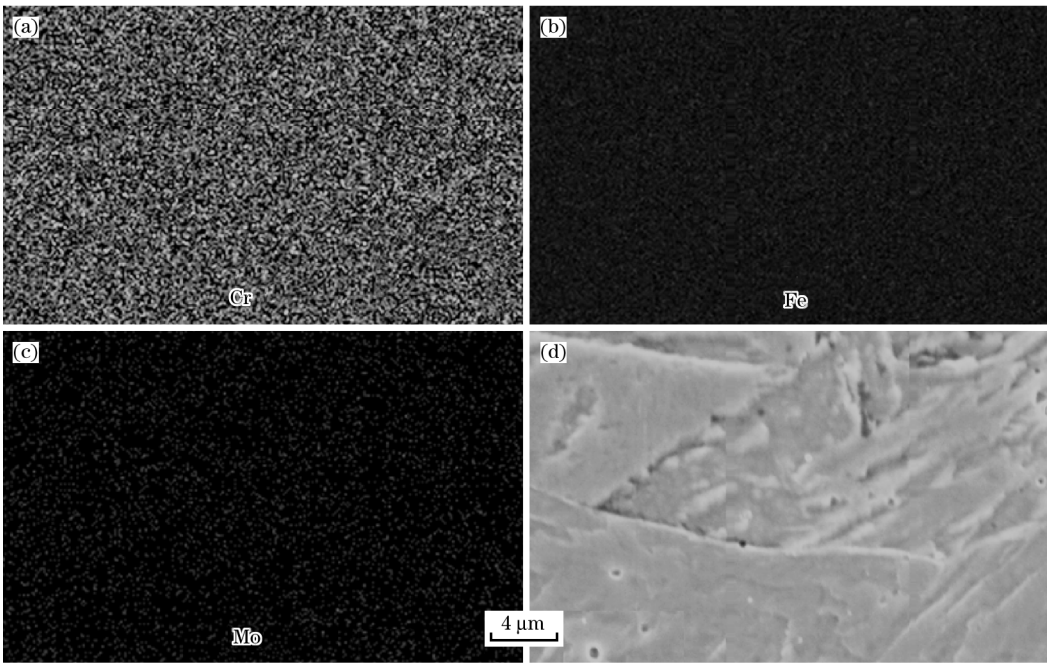

Fig. 4 Mapping of chemical composition in surface of machined sample C1 000+650+600

2.4 Hydrogen embrittlement

Regarding cathode charge HE tests, the behaviors of both samples were similar, that is to say tensile strength decreased and area reduction increased with the different PWHTs, in both conditions of hydrogen load. This last property was sensibly affected, according to P B Srinivasan et al[5], but it was not possible to detect differences in elongation values through the methods here utilized. The samples with highest hardness values were those more affected in this test, consistently with what was previously mentioned[29]. From these tests, variation of the area reduction could be quantified. The percentage value of ductility loss is used as the hydrogen embrittlement index, HEI[30]. It is given by

$$HEI=(AR_{air}-AR_{H})/AR_{air}\times 100\% \quad (1)$$

Table 2 presents the tensile property results in air and under hydrogen charging. It can be observed that ultimate tensile strength decreased under hydrogen charging. This fact shows the role played by hydrogen not only on ductility but also on this property[5].

It is well-known that hardness is one of the variables which control HE[29]: the higher the hardness, the higher the susceptibility to this degradation mechanism. In this sense, the PWHTs decreased the sensibility to HE because they decreased hardness (Table 2).

Fig. 5 shows SEM images of the fracture surface

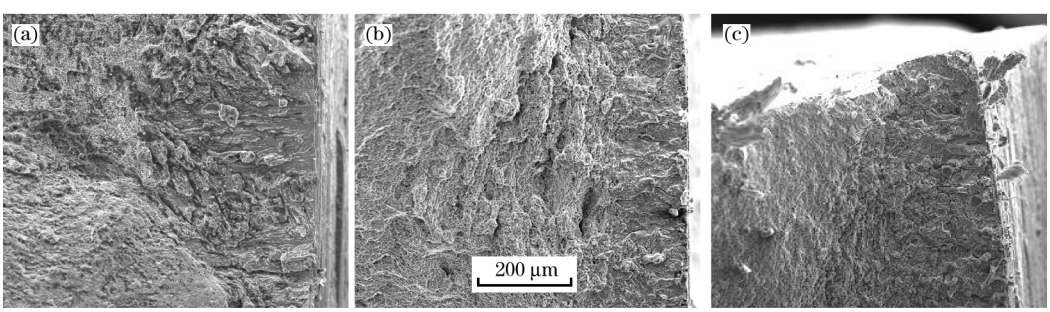

(a) Haw; (b) H1 000; (c) H1 000+650+600.

Fig. 5 SEM images of fracture surface of samples welded under Ar+5%He, tested under hydrogen conditions

of samples welded under Ar+5%He, tested under hydrogen conditions. The brittle layer thickness oscillated between 100 and 250 μm.

3 Discussion

The discussion of the chemical composition, microstructural characterization and mechanical properties of the samples analyzed in this study are reported in a previous paper[6].

3.1 PC resistance

Both chemical composition and microstructure have strong influence on the PC resistance[31]. The superficial passivity of stainless steels is associated with the presence of a chromium oxide layer. Pitting phenomenon is associated with the local rupture of this passive layer and then a higher stability of this layer will be related to a higher E_p, which is strongly affected by the chromium content. Mo and Cu can also increase the PC resistance, improving the cation-selective properties of the passive film and hindering the migration of aggressive anions, such as chlorides, to the metal surface or reducing the flux of cation vacancies in the passive film[31]; however, the exact mechanism is not clear yet. Samples welded under the Ar+18%CO_2 mixture presented lower Cr, Mo and Cu contents which could explain the lower E_p measured, due to a lower relative stability of the passive film.

Several studies have demonstrated that the kinetic of dissolution and the repassivation are controlled by Cr, Ni and Mo contents in the metal matrix[25]. In this sense, the slightly higher contents of Cr, Ni and Mo obtained in H specimens could explain the somewhat better performance of these samples.

Localized corrosion in passive metals is almost always initiated at local inhomogeneities as inclusions and precipitates or second phases, as well as in grain boundaries, dislocations and mechanical damaged places[9]. In this sense, it was observed that AW sample provided a structure less susceptible to this type of corrosion. Considering the PWHTs, the solubilizing and solubilizing plus double tempering treatments generated a decrease in E_p regarding the samples just AW, probably due to the presence of a sensitization phenomenon, which produces Cr depleted zones.

For the soft-martensitic steel, it is reported that an increase of retained austenite increases pitting corrosion resistance[25]. The explanation for this observation is related to the fact that this phase promotes dissolution of C and N and, in this way, avoids precipitation of these elements with Cr and Mo, generating a diminution of available sites for pit nucleation[9]. Nevertheless, Kimura reported no effect of retained austenite on E_p[32]. In this case, no direct effect of retained austenite was found [Fig. 1(b)]. AW and 1000+650+600 samples presented approximately the same austenite content and different E_p values. On the other hand, E_p of samples treated at 1000 ℃, with no ferrite and no austenite, were in between AW and 1000+650+600 samples.

Some authors[33] report that the presence of ferrite increases the susceptibility to pitting through promotion of the lower chromium content zone formation due to carbide precipitation. Other susceptible sites for pitting promotion are the primary austenite grain border or the tempered martensite matrix, where precipitation of carbide and/or carbonitrides can occur[9]. In this case, a positive effect of ferrite removal on E_p was not observed. Taking into account 1000+650+600 samples, for both shielding gases, where ferrite was eliminated and austenite was maximized, it was observed that E_p values were lower than those of the AW specimens. These results show that the deleterious effect of precipitation could have been more significant than the beneficial effect of both ferrite removal and austenite increase.

3.2 SCC tests

Although SMSS present good corrosion resistance behavior in sweet (CO_2) or slightly sour environments (low H_2S concentrations), the occurrence of IGSCC in HAZ of SMSS weldments, under certain medium conditions, has been reported[10]. In this work, IGSCC was not found but the treated samples showed IGC.

It was reported[12] that IGSCC in SMSS welds in test conditions was similar to those used in this work. The justification of this mechanism of corrosion is associated to a sensitization phenomenon generated by the decrease of Cr content due to the carbides precipitation in primary austenite grain boundaries. On the other hand, other authors[1,34] suggest that the mechanism of sensitization is associated with chromium oxide formation on the welding surface.

During the solubilizing heat treatment at 1000 ℃, segregation of Cr to the external Cr oxide layer and to the grain boundaries adjacent to the mentioned chromium oxide layer, was produced, generating an

impoverished in chromium area adjacent to the enriched in chromium grain boundaries. This impoverished in chromium area was more sensitive to corrosion than the matrix. A scheme of this mechanism can be seen in Fig. 6.

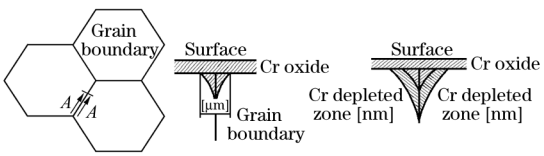

Fig. 6 Scheme of Cr segregation to Cr oxide external layer and to grain boundaries

3.3 Hydrogen embrittlement

In Fig. 7, HEI vs hardness values are shown. In this curve, it can be seen that susceptibility of this material was strongly dependent on hardness[29]. This relationship is an interesting technological result because it makes possible to estimate the loss of ductility under these conditions, knowing hardness values.

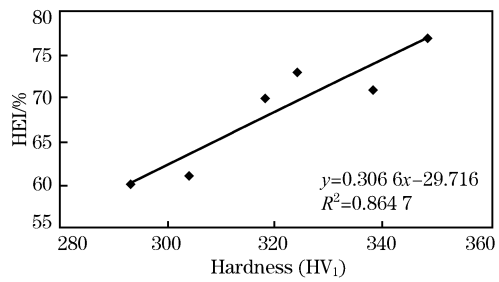

Fig. 7 Relationship between HEI and hardness

Other important factor that controls HE is the oxygen content of the welding deposit because it is known that inclusions are nucleation sites for hydrogen cracks[35]. Lower oxygen content implies lower inclusion contents, which imply higher resistance to this fail mechanism.

The differences in the retained austenite content obtained through the PWHTs, could affect HE because this phase is a potential tramp for hydrogen[36]. C Gesnouin et al[36] reported that the austenitic content could strongly affect this degradation mechanism because this phase tends to decrease the hydrogen permeation coefficient.

It is also reported[36] that for this type of steels, the generation of carbides and/or carbonitrides has a strong influence on hydrogen diffusion: the higher precipitate content, the lower hydrogen diffusion in the steel.

Comparing the two samples analyzed, it was observed that a little augmentation of C, N and O contents, corresponding to samples welded under CO_2 containing protection gas, provoked a slight increase in hydrogen susceptibility. The effect of PWHTs on hydrogen embrittlement index was related to microstructural conditions. That is to say that after solubilizing at 1000 ℃, during air cooling, a completely martensitic structure with carbides and/or carbonitrides precipitates was achieved. It was produced by low cooling velocity, with the elimination of the ferrite and austenite phases found in the AW sample. With the posterior solubilizing plus double tempering in air cooling, a tempered martensitic structure with both types of precipitates and high austenite content was reached, increasing in this way the resistance to this type of degradation.

The samples tested under hydrogen condition showed a flat fracture surface[5] (Fig. 5). Due to the fact that hydrogen was introduced in the sample by its surface, hydrogen concentration should be higher on it. That could explain why the crack starts at the surface, as is usually observed in these kinds of tests[30] and the final break in the center of the sample is ductile. The test rate does not give time for the HE mechanisms to develop and, as a consequence, last sector to break, breaks in a ductile mode[30]. The crack start was transgranular and the propagation followed different mechanisms depending on the material condition, with what in the periphery of the fracture surface, transgranular and intergranular fractures were evident[5,29].

4 Conclusions

1) The increase of oxidation potential in the shielding gas reduced resistance to PC due to the variations of chemical composition in the all weld metal and had no influence on the SCC, intergranular corrosion or hydrogen embrittlement behaviors.

2) The post weld heat treatments generated an increased susceptibility to pitting corrosion for both welded samples. The as-welded specimens provided a less susceptible microstructure to this mechanism of corrosion. The results obtained in this study showed no effect of the content of austenite, since the as-welded and 1000 + 650 + 600 treated specimens showed approximately the same content of retained austenite, but different E_p. Furthermore, samples heat treated at 1000 ℃ (without austenite or ferrite) had an intermediate E_p under both conditions.

3) The post weld heat treatments did not influence the SCC behaviors as it was not found in any

sample under study. However, there was evidence of IGC associated with segregation, essentially of Cr, in primary austenite grain boundary generated by surface oxidation during thermal cycling.

4) The post weld heat treatments produced variation in the HEI. As hardness decreased, reduction of area increased for all conditions under hydrogen charging. The specimens with higher hardness values were the most susceptible to hydrogen damage. Tensile property decreased under the hydrogen condition.

The authors wish to express their gratitude to ESAB-Sweden for the donation of the consumable and LECO chemical analysis, to CONARCO-ESAB-Argentina for performing chemical analysis, to AIR LIQUIDE Argentina for donating the welding gases, to the LATIN AMERICAN WELDING FUNDATION, Argentina, for facilities for welding and mechanical testing, to the Scanning Electron Microscopy Laboratory of INTI-Mechanics, Argentina, for facilities for SEM analysis and to both APUEMFI, Argentina and ANPCyT, Argentina for financial support.

References:

[1] Amaya H, Kondo K, Taniyama A, et al. Stress Corrosion Cracking Sensitivity of Super Martensitic Stainless Steel in High Chloride Concentration Environment [C] // Corrosion 2004. Houston: NACE International, 2004: 04124.

[2] Van der Winden H, Toussaint P, Coudreuse L. Past, Present and Future of Weldable Supermartensitic Alloys [C] // Supermartensitic 2002. Brussels: Stainless Steel Word, 2002: 9.

[3] Bilmes P, Llorente C, Solari M. Role of the Retained Austenite on the Mechanical Properties of 13Cr-4NiMo Weld Metals [C] // The 20th ASM Heat Treating Society. Missouri: ASM, 2000: 556.

[4] Karlsson L, Rigdal S, Bruins W, et al. Efficient Welding of Supermartensitic Stainless Steels With Matching Composition Consumables [C] // Stainless Steel Word. The Hague: Stainless Steel Word, 1999: 341.

[5] Srinivasan P, Sharkawy S, Dietzel W. Hydrogen Assisted Stress-Cracking Behavior of Electron Beam Welded Supermartensitic Stainless Steel Weldments [J]. Materials Science and Engineering, 2004, 385A(1/2): 6.

[6] Zappa S, Svoboda H, Ramini M, et al. Improving Supermartensitic Stainless Steel Weld Metal Toughness [J]. Welding Journal, 2012, 91(3): 83s.

[7] Bilmes P, Solari M, Llorente C. Characteristics and Effect of Austenite Resulting From Tempering of 13Cr-NiMo Martensitic Steel Weld Metals [J]. Materials Characterization, 2001, 46(4): 285.

[8] Bilmes P. Role of the Austenite on the Mechanical Properties of Soft Martensitic Stainless Steels Weld Metals [D]. La Plata: Universidad Nacional de La Plata, 2000.

[9] Aquino J, Rovere C, Kuri S. Localized Corrosion Susceptibility of Supermartensitic Stainless Steel in Welded Joints [J]. Corrosion Science, 2007, 51(10): 2323.

[10] Amaya H, Taniyama A, Ogawa K. Intergranular Stress Corrosion Cracking Susceptibility and Precipitation Behaviour on Grain Boundary by Post Weld Heat Treatment of Super Martensitic Stainless Steels [C] // Corrosion 2008. Houston: NACE International, 2008: 08100.

[11] Hashizume S, Nakayama T, Sakairi M, et al. Electrochemical Behavior of Low C-13% Cr Weld Joints by Using Solution Flow Type Micro-droplet Cell [C] // Corrosion 2008. Houston: NACE International, 2008: 08102.

[12] Miyata Y, Kimura M. Effects of Thermal Cycle Conditions on Intergranular Stress Corrosion Cracking in Sweet Environment for Supermartensitic Stainless Steel [C] // Corrosion 2005. Houston: NACE International, 2005: 05095.

[13] Zappa S, Svoboda H, Ramini M, et al. Effect of Shielding Gas on the Properties of Supermartensitic Stainless Steel All Weld Metal [C] // CONAMET-SAM 2006. Santiago de Chile: CONAMET-SAM, 2006.

[14] Lippold J, Kotecki D. Welding Metallurgy and Weldability of Stainless Steels [M]. New Jersey: John Wiley and Sons, 2005.

[15] Kimura M, Miyata Y, Toyooka T, et al. Effect of Test Method on SSC Performance of Modified 13Cr Steel [C] // Corrosion 1998. Houston: NACE International, 1998: 98114.

[16] Hara T, Asahi H. Conditions Under Which Cracks Occur in Modified 13% Chromium Steel in Wet Hydrogen Sulfide Environments [C] // Corrosion 2000. Houston: NACE International, 2000: 00050533.

[17] ANSI/AWS A5.22—95, Specification for Stainless Steel Electrodes for Flux Cored Arc Welding and Stainless Steel Flux Cored Rods for Gas Tungsten Arc Welding [S]. Miami: American Welding Society, 1995.

[18] ANSIB31.3—96, Chemical Plant and Petroleum Refinery Piping [S]. Miami: American National Standards Institute, 1996.

[19] ASTM E562—99, Standard Test Method for Determining Volume Fraction by Systematic Manual Point Count [S]. Miami, ASTM International, 1999.

[20] Cullity B, Stock S. Elements of X Ray Diffraction [M]. 3rd ed. New Jersey: Prentice Hall, 2001.

[21] Bilmes P, Llorente C, Desimone J, et al. Microstructures and Properties of Martensitic Stainless Steels of 13% Cr-4% NiMo Weld Metals FCAW [C] // II Encuentro de Ingeniería de Materiales. La Habana: 1998: 252.

[22] Zappa S, Svoboda H, Ramini M, et al. Effect of Post Weld Heat Treatment on the Properties of a Supermartensitic Stainless Steel Welded With a Tubular Metal-Cored Wire [J]. Soldagem e Inspecão. 2007, 12(2): 115.

[23] Baroux B, Marcus P. Corrosion Mechanism in Theory and Practice [M]. 2nd ed. New York: [s. n.], 2002.

[24] Shibata T, Takeyama T. Stochastic Theory of Pitting Corrosion [J]. Corrosion, 1977, 33(7): 243.

[25] Bilmes P, Llorente C, Huamán L, et al. Microstructure and Pitting Corrosion of 13CrNiMo Weld Metals [J]. Corrosion Science, 2006, 48(10): 3261.

[26] Shibata T. Uhlig's Corrosion Handbook [M]. 2nd ed. New York: [s. n.], 2000.

[27] NACE TM0177—05. Laboratory Testing of Metals for Resistance to Sulfide Stress Cracking and Stress Corrosion Cracking in H2S Environments [S]. Miami: NACE International, 2005.

[28] EFC 17. Corrosion Resistant Alloys for Oil and Gas Production Guidance on General Requirements and Test Methods for

H_2S Service [M]. 2nd ed. London: Maney Publishing, 1996.

[29] Srinivasan P, Sharkawy S, Dietzel W. Environmental Cracking Behavior of Submerged Arc-Welded Supermartensitic Stainless Steel Weldments [J]. Journal of Materials Engineering and Performance, 2004, 13(2): 232.

[30] Hazarabedian A, Bilmes P, Llorente C, et al. Effect of Post Weld Heat Treatments on the Damage Hydrogen Resistance of "Soft Martensitic" Stainless Steels Weld Metals [C] // SAM-CONAMET 2003. San Carlos de Bariloche: SAM-CONAMET, 2003: 242.

[31] Bohni H. Uhlig's Corrosion Handbook [M]. 2nd ed. Zurich: [s. n.], 2000.

[32] Kimura M, Miyata Y, Toyooka T. Effect of Retained Austenite on Corrosion Performance for Modified 13%Cr Steel Pipe [J]. Corrosion, 2000, 57(5): 01050433.

[33] Hara T, Asahi H. Effect of Delta-Ferrite on Sulfide Stress Cracking in a Low Carbon 13 mass% Chromium Steel [J]. ISIJ International, 2000, 40(11): 1134.

[34] Woollin P. Post Weld Heat Treatment to Avoid Intergranular Stress Corrosion Cracking of Supermartensitic Stainless Steels [J]. Welding in the Word, 2005, 51(9/10): 31.

[35] Beghini M, Benamati G, Bertini L, et al. Effect of Hydrogen on Tensile Properties of Martensitic Steel for Fusion Application [J]. Journal of Nuclear Materials, 1998, 258-263: 1295.

[36] Gesnouin C, Hazarabedian A, Bruzzoni P, et al. Effect of Post-Weld Heat Treatment on the Microstructure and Hydrogen Permeation of 13CrNiMo Steels [J]. Corrosion Science, 2004, 46(7): 1633.